JOURNAL OF PHYSICAL ORGANIC CHEMISTRY
J. Phys. Org. Chem. 2005; **18:** 800–817
Published online 23 May 2005 in Wiley InterScience (www.interscience.wiley.com). DOI: 10.1002/poc.945

Vinyl or isopropenyl substituents as experimental and theoretical probes for diamagnetic anisotropies of aromatic hydrocarbons†

Guenter Haefelinger,* Wolfgang Knapp, Thomas Zuschneid and Frank Peter Dietrich

University of Tübingen, Institute of Organic Chemistry, Auf der Morgenstelle 18, D-72076 Tübingen, Germany

Received 26 February 2005; revised 22 March 2005; accepted 29 March 2005

ABSTRACT: Vinyl or isopropenyl substituents can be used to indicate anisotropy effects in the surroundings of benzenoid hydrocarbons by experiments together with APUDI model and *ab initio* GIAO MO calculations from the difference in geminal proton splittings of the olefinic substituents. Geometry optimizations as a function of the torsional angle between substituents and aromatic planes were performed in two polarized basis sets for the HF, B3LYP and MP2 methods. Calculated splittings range between −0.70 and 0.48 ppm. Comparison with experimental ^{1}H NMR shifts does not lead precisely to the determination of the experimentally apparent effective torsional angle.

KEYWORDS: vinyl substituents; isopropenyl substituents; torsional dependence; *ab initio* geometry optimizations; GIAO; ^{1}H NMR shieldings; vinylic protons; experimental splittings; APUDI splittings; geminal H signals

INTRODUCTION

Aromaticity[1–5] is a theoretical concept of organic chemistry which is of immense practical importance[6] and which has lately found renewed interest.[7,8] Aromaticity is reflected in an unexpected (unusual) stability of cyclically conjugated unsaturated organic compounds yielding special properties in various fields. After introduction of the cyclic benzenoid formula by Kekulé[9] in 1865, the reactivity with typical electrophilic substitution instead of the expected addition[10] to double bonds was the first important descriptor of aromatic behaviour. However, this depends on the energetic difference between the ground state and the activation barrier towards the transition state of Wheland's intermediate σ-complex.[11] Today aromaticity is considered as a pure ground-state property. Most criteria of aromaticity depend critically on the selection of a reference state and therefore aromaticity may be termed an excess property.

CRITERIA OF AROMATICITY

Properties of aromatic compounds may be defined by the following criteria:

1. *Electronic structure of cyclically conjugated π-systems:* After formulation of the important role of the aromatic sextet of electrons by Armit and Robinson,[12] its extension by Hückel's rule[13] classified planar, monocyclic, unsaturated conjugated organic hydrocarbons as aromatic if they contain $(4n + 2)$ π-electrons.[14]
2. *Energetic stabilization:* Aromatic molecules show unusually high energetic stabilization[15] deviating from additive bond energy models. This was shown experimentally by heats of formation[16] or via hydrogenation energies.[17] Theoretically the term resonance energy (RE) was defined in the first in π-electron valence bond (VB) theory.[18] In the Hückel molecular orbital (HMO) method, delocalization energies were converted to theoretical energy criteria: REPE (resonance energy per electron) by Hess and Schad,[19] the specific π-bond energy[20] in our group and Dewar's resonance energy[21] by HMO[22] and Pariser–Parr–Pople (PPP)[23] treatments. *Ab initio*-calculated total energies lead via comparison with specifically defined reference molecules to isodesmic,[24] homodesmotic[25] or superhomodesmotic[26] energies termed aromatic stabilization energies (ASEs).[27]
3. *Molecular structure:* Aromatic molecules show a tendency for equalization of CC bond lengths[28] intermediate between single and double bonds. This led Krygowski and co-workers to the definition of the harmonic oscillator model of aromaticity (HOMA),[29] which can be applied globally or locally for individual rings of polycyclic and also heterocyclic systems. This descriptor of aromaticity is derived from energy

**Correspondence to:* G. Haefelinger, University of Tübingen, Institute of Organic Chemistry, Auf der Morgenstelle 18, D-72076 Tübingen, Germany.
E-mail: guenter.haefelinger@uni-tuebingen.de
†Selected paper presented for a special issue dedicated to Professor Otto Exner on the occasion of his 80th birthday.

(based on a harmonic approximation named the HOSE[30] model) but determined solely by variations in distances. Other purely geometric criteria are A_J values introduced by Julg and Francois[31] and I_6 values of Bird.[32]

4. *Magnetic properties:* Owing to induction of ring currents[33] in the cyclic π-system, aromatic compounds show a peculiar behaviour in magnetic fields. This leads to strong anisotropy[34] and enhancement (exaltation)[35] of diamagnetic susceptibility[36] proposed as criteria of aromaticity. In the ^{1}H NMR spectrum due to the opposite orientation of the induced ring current (as shown in Fig. 1), a characteristic low-field shift (deshielding effect) of exocyclic ring protons is observed.[37] Protons located inside or above the ring plane are high-field shifted[38] (shielding effect). This general behaviour of aromatic compounds was termed diatropicity by Elvidge and Jackman.[39] As a purely theoretical property, Schleyer *et al.* introduced nuclear independent chemical shifts (NICSs),[40] which are negative values of *ab initio* GIAO MO[41] calculated chemical shifts at the centre of the considered ring or 1.0 Å above that position [NICS(1)].

We concentrate here on the diamagnetic ring current effect in the ^{1}H NMR spectrum as a very important ground-state indicator of aromaticity and want to show how one can use a vinyl or isopropenyl substituent on benzenoid hydrocarbons as a measure of ring current-induced anisotropies. We present the synthesis, experimental high-field ^{1}H NMR data, *ab initio* MO optimizations in two basis sets and three theoretical models of the torsional dependence of geometries and also total energies and GIAO-calculated chemical shifts of geminal vinylic protons (see Scheme 2) in comparison with APUDI model predictions.

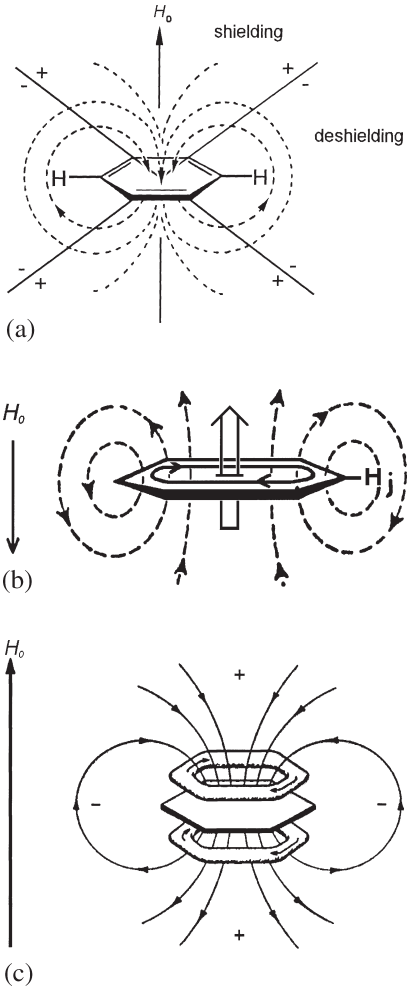

Figure 1. (a) Qualitative ring current anisotropies with shielding and deshielding regions. The zero line cone is oriented at the 'magic angle' of MAS spectroscopy of 54.7° derived from the McConnell equation. (b) Pople's point dipole model. (c) Two-loop model of Waugh and Fessenden. The loop separation is 1.28 Å

QUANTITATIVE MODELS OF RING CURRENTS[42]

Such models allow the calculation of the ^{1}H NMR chemical shifts of the ring protons of benzenoid hydrocarbons or the influence of test protons which are geometrically located in the neighbourhood of a benzene ring, as shown schematically in Fig. 1(a).

The first calculation of the ring current of benzene is due to Pople,[43] who located a point dipole in the middle of the benzene ring and determined its geometric dependence by the classical equation of McConnell,[44] as shown in Fig. 1(b). Extensions to a two-loop model [see Fig. 1(c)] were presented by Waugh and Fessenden[45] and also by Johnson and Bovey,[46] providing tables of iso-shielding lines[47] by use of elliptic integrals. Similar tables based on the London[48]–McWeeny[49] HMO model have been presented by Haigh and Mallion.[50] In an extension of Pople's first model, we introduced an additive atomic point dipole model[51] called the APUDI (Atomares Punkt-Dipol) model. Similar additive models have been developed by Barfield *et al.*[52] and by Blustin.[53] Advanced coupled HF procedures were developed consecutively.[54–57] However, since the 1990s chemical shifts could be calculated directly by *ab initio* GIAO MO calculations[41] with reasonable accuracy,[58] which will be applied here for the vinyl- and isopropenyl-substituted systems in comparison with results of the APUDI model.

EXPERIMENTAL DETERMINATIONS OF RING CURRENT ANISOTROPIES

The ^{1}H NMR signals of the protons of benzene are shifted to low field by 1.68 ppm with respect to the olefinic standard cyclohexene.[59] Low-temperature spectra of large monocyclic Hückel aromatic $(4n + 2)$ π-annulenes show

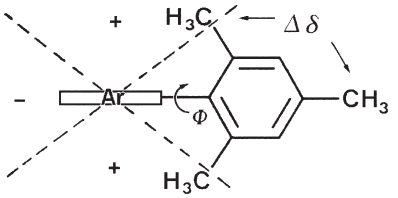

Scheme 1. Splitting ($\Delta\delta$) of *o,p*-methyl group signals of mesityl-substituted aromatic compounds

low-field signals for exocyclic protons and high-field shifts for endocyclic protons.[38] This effect is also observed in Vogel's methylene bridged [10]- and [14]-annulenes.[60] Especially interesting is the situation in *para*-bridged [*n*]-paracyclophanes,[61] where a polymethylene chain bridges the 1,4-positions of a benzene ring which is distorted strongly from planarity for small ($n = 4$ and 5) up to nearly planar rings for $n = 8$–10.

o,p-METHYL GROUP SIGNAL SPLITTING ($\Delta\delta$) OF MESITYL-SUBSTITUTED BENZENOIDS

Musso and co-workers[62] introduced, at the end of the 1960s, the use of mesityl substituents on aromatic systems as an indicator for ring current anisotropies, which was also studied in our group.[63] The *p*-methyl group signal serves as an internal standard (which is only weakly influenced by the ring current) towards the signal of the two identical *o*-methyl group protons which are geometrically located in the high-field anisotropy cone of the parent hydrocarbon, as shown in Scheme 1. The resulting splitting of the *o,p*-methyl group singlet signals is a simple and unambiguous qualitative ring current probe which was independent of the limited reproducibility of the continuous wave (CW) NMR spectrometers of that time. The magnitude of the splitting is dependent on the torsional angle Φ between the aromatic system and the mesityl substituent. This value is 0.313 ppm for phenylmesitylene with an experimental torsional angle determined by electron diffraction[64] of $\Phi = 77.5°$ and 0.463 ppm for bimesityl with assumed $\Phi = 90°$. The splitting is also dependent on the kind and position of the studied benzenoid system. Splitting values for 2- and 1-mesitylnaphthalene are 0.33 and 0.51 ppm, respectively. A maximum value of 0.744 ppm is obtained for 9-mesitylanthracene.[62]

An experimental disadvantage is the difficult synthesis of mesityl-substituted compounds. For quantitative evaluation of the splitting, the torsional angle Φ has to be determined by calculation or by experiment. Another difficulty results from the large rotational cone of the methyl group in the ring current anisotropy field, as shown in Fig. 2 for a 90° orientation of Φ inserted into the Haigh–Mallion iso-shielding plot. The *o*-methyl proton shifts span a range from 0.40 to 0.05 ppm, which have to be averaged for quantitative comparison with the experimental splitting.

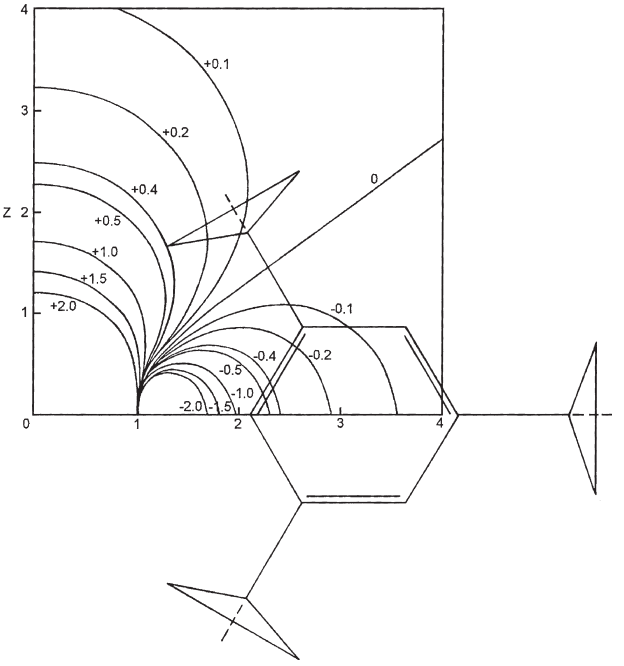

Figure 2. Mesityl group splitting and mesityl substituent oriented perpendicular in scale to the plot of Haigh–Mallion iso-shielding lines of benzene

SPLITTING OF GEMINAL PROTONS OF VINYL- OR ISOPROPENYL-SUBSTITUTED BENZENOIDS

To avoid the disadvantages of the mesityl substituent, we suggest here the use of a vinyl or isopropenyl substituent as a ring current probe, looking for the size of the splitting ($\Delta\delta$) of the geminal protons ($H_a - H_b$) in different aromatic systems as shown in Scheme 2. The geometric position of these hydrogens is more precisely located and mainly determined by the torsional twist angle Φ between the planar vinylic substituent and the planar aromatic system.

The synthesis of such compounds is much easier but the resulting NMR spectra are more complicated owing to spin–spin coupling, requiring high-field NMR spectrometers. Molecular geometries and torsional dependences of such compounds can be calculated reliable by *ab initio* gradient optimizations which can be extended to direct GIAO MO calculations of corresponding chemical shifts. These calculated shifts will be compared with APUDI model predictions and with experimental values.

PROCEDURES OF CALCULATIONS

Ab initio MO optimizations of molecular geometries of molecules **1a**–**5a**, **8a** and **1b** shown in Scheme 2 were performed by use of the Gaussian 03 program system[65] for each torsional angle Φ in steps of 15° (except **8a**) from 0° to 90° or 180° if necessary from symmetry. Planarity

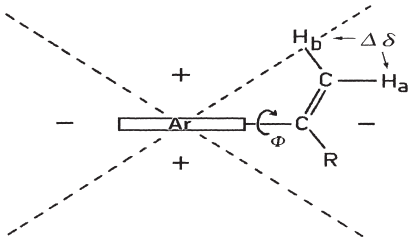

a: R = H vinyl derivatives		b: R = CH_3 isopropenyl derivatives	
No.	Vinylarenes	No.	Isopropenylarenes
1a	styrene	**1b**	isopropenylbenzene[a]
2a	2-methylstyrene[b]	**2b**	2-methylisopropenylbenzene[c]
3a	2,6-dimethylstyrene[d]	**3b**	2,6-dimethylisopropenylbenzene[e]
4a	2-vinylnaphthalene[f]	**4b**	2-isopropenylnaphthalene[g]
5a	1-vinylnaphthalene[f]	**5b**	1-isopropenylnaphthalene[g]
6a	2-vinylanthracene[f]	**6b**	2-isopropenylanthracene[h]
7a	1-vinylanthracene[f]	**7b**	1-isopropenylanthracene[i]
8a	9-vinylanthracene[f]	**8a**	9-isopropenylanthracene[j]
9a	9-vinylphenanthrene[f]	**9b**	9-isopopenylphenanthrene[f]
10a	1-vinylpyrene[f]		
11a	6-vinylchrysene[f]		

[a]Staudinger H, Breusch F. *Ber. Dtsch Chem. Ges.* 1929; **62**: 442.
[b]Bilas W, Duschel C, Schmidt H. *J. Prakt. Chem.* 1973; **305**: 88.
[c]Hirschberg Y. *J. Am. Chem. Soc.* 1949; **71**: 3241.
[d]Schwartzmann H, Corson BB. *J. Am. Chem. Soc.* 1954; **76**: 781.
[e]Schloman WW, Morrison H. *J. Am. Chem. Soc.* 1977; **99**: 3342.
[f]Church DF, Gleicher GJ. *J. Org. Chem.* 1976; **41**: 2327.
[g]Dewar MJS, Sampson RJ. *J. Chem. Soc.* 1976; 2952.
[h]Stola M, Yanus JF, Pearson JM. *Macromolecules* 1976; **9**: 710.
[i]Stola M, Yanus JF, Pearson JM. *Macromolecules* 1976; **9**: 715.
[j]Coudanne J, Maréchal E. *C. R. Acad. Sci., Ser. C* 1978; **286**: 169.

Scheme 2. Names, numbering and references to synthesis of the considered vinyl- and isopropenyl-substituted compounds

was imposed on the aromatic systems and the vinylic substituents. The status of the conformers was checked by frequency calculations. We used the single determinant restricted Hartree–Fock (HF) model[66] with Pople's 6–31G* double-zeta split valence basis set,[67] which has polarization d-functions on carbon, and with the larger correlation consistent polarized triple-zeta cc-pVTZ basis set of Dunning,[68] which has polarization functions on carbon and hydrogen for calculations of only **1a**–**3a** and **1b**. In an extension of this, density functional theory (DFT)[69] calculations with the often applied hybrid, semilocal gradient-corrected density functional (B3LYP)[70] were performed in both basis sets for the same molecules. As post-HF perturbative method of second-order Møller–Plesset (MP2)[71] calculations were applied for **1a** and **1b** to estimate the influence of electron correlation with 6–31G* and 6–311G* basis sets.

SYNTHESIS

Molecular formulae and notations of the molecules studied here are presented in Scheme 2. All of these compounds are already known experimentally and had been prepared partly by us for NMR measurements. They can be easily obtained from the corresponding acetophenones. From these the vinyl derivatives **1a**–**11a** may be obtained via $LiAlH_4$ reduction to carbinols and consecutive dehydration. Isopropenyl substances **1b**–**9b** can be synthesized from acetophenones via Wittig reaction with methylenetriphenylphosphoniumylide. Experimental details can be found in the thesis of Knapp.[72]

RESULTS AND DISCUSSION

Experimental ^{1}H NMR spectra

^{1}H NMR spectra were recorded in $CDCl_3$ at 90 or 400 MHz with Bruker WH 90 or 400 MHz FT instruments and are referenced to internal TMS. Spectra of **9b** and all vinylic systems except **2a** and **3a** are taken from Church and Gleicher,[73] which were run in $CDCl_3$ on Varian HA-100 or EM-360 spectrometers.

The vinyl substituents show a spin-coupled AMX spectrum which is resolved at 90 MHz into a quartet for each of the three proton signals H_a, H_b and H_c with a $^3J_{cis}$ and $^3J_{trans}$ coupling of H_c to H_a and H_b and the geminal ^2J coupling between H_a and H_b.

The isopropenyl substituents show free rotation of the three equivalent methyl group protons, which leads to an AMX_3 spin-coupling pattern. The methyl group signal is split into two doublets via ^4J coupling to H_a and H_b and their signals occur each as separate quartets due to ^4J methyl group coupling. The splitting patterns are shown schematically in Fig. 3 with the experimental spectrum of **3b** as an example.

Experimental data are given in Table 1 for aromatic vinyl systems and in Table 2 for isopropenyl derivatives. Coupling constants taken from experiments directly are less precisely determined than chemical shifts.

For vinyl groups, all three types of vinylic protons (H_a, H_b and H_c) vary in an appreciable range up to 0.9 ppm, which is apparently dependent on the estimated torsional angle Φ between the arene nucleus and the vinyl substituent. These chemical shifts are influenced by a small or zero torsional angle in styrene (**1a**) and in the 2-vinyl-substituted systems of naphthalene (**4a**) or anthracene (**6a**) to an intermediate value in **2a** caused by the steric effect of *o*-methyl substitution or in the sterically affected 1-positions in 1-naphthalene (**5a**), 1-anthracene (**7a**) and in 9-phenanthrene (**9a**), 1-pyrene (**10a**) and 6-chrysene (**11a**) where the differences should be caused by the aromatic system for a nearly constant $\Phi \neq 0°$. A nearly perpendicular orientation may be assumed in the *o*,*o*′-dimethyl-substituted styrene (**3a**) and in 9-anthracene (**8a**).

The advantage of the isopropenyl substituent in comparison with the vinyl group is that the parent compound **1b** should be appreciably twisted and consecutively all derivatives **2b**–**9b** will show increased torsional angles Φ towards a perpendicular orientation. The influence from the isopropenyl methyl group should be independent of Φ.

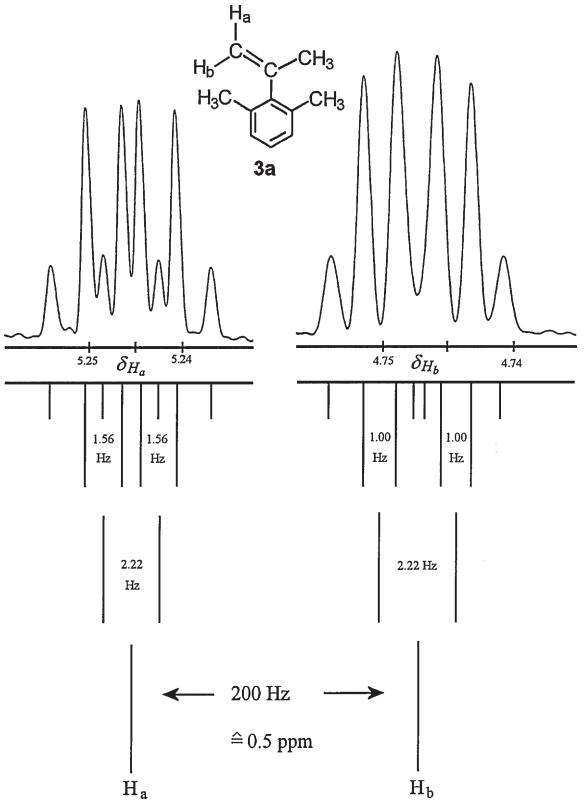

Figure 3. Experimental ^{1}H NMR spectrum of **3a** at 400 MHz and splitting patterns of couplings in isopropenyl substituents (different scale expansions)

The experimentally derived splittings of geminal protons (last columns in Tables 1 and 2) span a range from −0.53 to +0.62 ppm. Positive splittings of vinyl systems in Table 1 are only observed for **3a** and **8a** but more often for isopropenyl systems in Table 2. The reference signal of H_a is not constant, but strongly dependent on Φ.

Any further consideration needs first the determination of geometric details, especially the behaviour of the potential energy curve as a function of Φ.

Geometry optimizations with basis set and method dependence of total energies in dependence on torsional angles Φ

Vinyl systems

*Styrene (***1a***).* Torsional angles (Φ_{min}) at minimum energy conformations of styrene (**1a**) and internal barriers to rotations towards $\Phi = 90°$ have been reported several times by *ab initio* HF gradient optimizations in various basis sets (such as Pople's basis sets: STO-3G, 4–21G, 4–31G, 6–31G and 6–31G*) with references to literature results collected by Tsuzuki *et al.*[74] The minimum energy torsional angle Φ_{min} was calculated as unequal to zero only for 4–21G as $\Phi_{min} = 24°$ and 4–31G as $\Phi_{min} = 18°$ (both in Ref. 75) and for 6–31G* as $\Phi_{min} = 15°$ (Ref. 74).

A constant HF/6–31G* derived geometry decreases the barrier height at $\Phi = 90°$ from the HF value of 2.88 kcal mol^{-1} for three MP calculations to 2.61 kcal mol^{-1} for MP2 and MP3 to 2.48 kcal mol^{-1} with MP4(SDQ)[74] (1 kcal = 4.184 kJ). Five differently derived experimental maximum barrier heights at $\Phi = 90°$ cited in Table 4 range between 1.78[76] and 3.29 kcal mol^{-1}.[77]

The results of our optimizations of **1a** for each torsional angle are presented in Table 3. Our HF/6–31G* optimization leads, contrary to the 15° in Ref. 74, to a minimum torsional angle of $\Phi_{min} = 21.76°$. In that study,[74] **1a** had been optimized without any constraint, i.e. no planarity of the phenyl ring and the vinyl substituent was imposed. This led to a total energy of −307.58546 hartree, which is slightly lower than our value of −307.5819 hartree presented in Table 3 (in Tables 3 and 5–7 are minimum torsional angles and corresponding total energies listed in the last rows in units of hartrees = 627.5095 kcal mol^{-1} in comparison with literature values where available). Our HF calculation with the larger cc-pVTZ basis set leads to a lower value of $\Phi_{min} = 16.37°$, but both B3LYP calculations give $\Phi_{min} = 0.0°$. The MP2 optimizations yield $\Phi_{min} = 28.55°$

Table 1. Experimental ^{1}H NMR chemical shifts, δ (ppm), and coupling constants, *J* (Hz), of vinyl-substituted benzenoids in $CDCl_3$ with internal TMS at 90 MHz

Compound	δH_a	δH_b	δH_c	J_{ab}	J_{ac}	J_{bc}	$\Delta\delta(H_a - H_b)$
1[a]	5.244	5.744	6.737	1.03	10.81	17.59	−0.500
1a[a]	5.16	5.66	—	1.0	10	18	−0.50
2[a]	5.277	5.621	6.945	1.47	11.04	17.52	−0.344
3[a]	5.526	5.248	6.691	2.05	11.44	17.89	0.278
4a[a]	5.25	5.75	6.80	1.0	10	18	−0.50
5a[a]	5.36	5.65	—	1.5	10	18	−0.29
6a[a]	5.40	5.93	6.97	1.0	11	17	−0.53
7a[a]	5.41	5.74	—	1.5	11	17	−0.33
8a[a]	6.00	5.63	—	2.0	11	17	0.37
9a[a]	5.35	5.69	—	2.0	11	16	−0.34
10a[a]	5.44	5.87	—	2.0	11	17	−0.38
11a[a]	5.60	6.00	—	2.0	11	17	−0.40

[a] Ref. 73.

Table 2. Experimental ^{1}H NMR chemical shifts, δ (ppm), and coupling constants, J (Hz) of isopropenyl-substituted benzenoids in $CDCl_3$ with internal TMS at 400 MHz

Compound	δH_a	δH_b	δCH_3	J_{ab}	J_{ac}	$J_{b\,Me}$	$\Delta\delta(H_a - H_b)$
1b	5.079	5.361	2.152	1.57	1.51	0.82	−0.282
2b	5.182	4.837	2.031	2.22	1.56	0.93	0.345
3b	5.252	4.754	1.048	2.22	1.56	1.00	0.498
4b	5.188	5.525	2.263	1.47	0.77	1.50	−0.337
4b[a]	5.10	5.50	2.20	—	—	—	−0.40
5b	5.401	5.056	2.205	1.57	0.96	2.24	0.345
5b[a]	5.35	5.00	2.16	—	—	—	0.35
6b	5.247	5.611	2.310	1.42	0.80	1.43	−0.364
7b	5.438	5.146	2.239	1.47	1.02	2.17	0.292
8b	5.752	5.130	2.262	1.54	1.03	2.23	0.622
9b[a]	5.10	5.30	2.15	—	—	—	−0.20

[a] Ref. 73.

Table 3. Basis set and method dependence of optimized potential energies ΔE (kcal mol^{-1}) relative to E_{min} for styrene (**1a**) as a function of the torsional angle Φ[a]

Angle Φ(°)	ΔE HF/ 6–31G*	ΔE[a] HF/ 6–31G*	ΔE HF/ cc-pVTZ	ΔE B3LYP 6–31G*	ΔE B3LYP cc-pVTZ	ΔE MP2/6–31G*	ΔE MP2/6–311G*
0	0.088	0.041	0.026	0.000	0.000	0.316	0.462
15	0.023	0.000	0.001	0.064	0.053	0.154	0.253
30	0.056	0.173	0.114	0.436	0.396	0.003	0.002
45	0.549	0.713	0.656	1.363	1.250	0.394	0.274
60	1.468	1.637	1.561	2.665	2.455	1.321	1.081
75	2.352	2.522	2.404	3.787	3.499	2.240	1.901
90	2.713	2.884	2.744	4.223	3.908	2.614	2.236
Φ_{min}(°)	21.76	15.02	16.37	0.00	0.00	28.55	31.42
E_{min} (hatree)	−307.58519	−307.58546	−307.68850	−309.64796	−309.76000	−308.59325	−308.59325

[a] Ref. 73, HF/6–31G* $\Delta E_{0°} = 0.04$ kcal mol^{-1}, $\Delta E_{90°} = 2.88$ kcal mol^{-1}; Ref. 72, HF/STO-3G $\Phi_{min} = 0.0°$, $E_{min} = -303.83445$, $\Delta E_{90°} = 4.54$ kcal mol^{-1}.

with 6–31G* and $\Phi_{min} = 31.42°$ with the larger 6–311G* basis set. (We could not perform an MP2/cc-pVTZ optimization of **1a** because of limitations of our computer facilities.)

The torsional dependence of potential energies for all three applied methods with triple zeta basis sets is shown in Fig. 4.

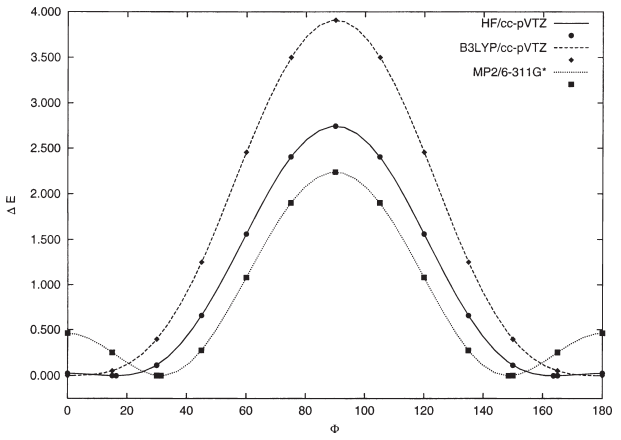

Figure 4. Potential energies (kcal mol^{-1}) of styrene (**1a**) as a function of the torsional angle Φ from HF/cc-pVTZ, B3LYP/cc-pVTZ and MP2/6–311G* optimizations

Calculated maximum barrier heights at $\Phi = 90°$ are fairly uniform for both HF optimizations, 2.71 and 2.74 kcal mol^{-1}, larger for B3LYP, 4.22 and 3.91 kcal mol^{-1} for 6–31G* and cc-pVTZ basis sets, and intermediate values from MP2 calculations, 2.61 and 2.24 kcal mol^{-1} for 6–31G* and 6–311G* basis sets.

The energies in Table 3 refer to a minimum path for variation with Φ which is not observed experimentally. These values are denoted by E° in Table 4 where we present additionally zero point vibration energy corrections (E_{ZP}) and thermal energy corrections (E_{Th}) to E° which are derived from 6–31G* frequency calculations. These values are unequal for each rotational angle Φ and for each method.

Such corrections for **1a** lower in each method the 90° barrier, in the HF method from 2.71 to 2.46 or 2.00 kcal mol^{-1}. The B3LYP barriers are larger, 4.22 to 4.04 and 4.01 kcal mol^{-1}, and the MP2 barriers range from 2.61 to 2.53 and 2.07 kcal mol^{-1}. Unfortunately, these corrected barriers do not increase the agreement to the five experimental values given in Table 4; they are too low.

The predicted second rotational barrier at $\Phi = 0°$ is small, 0.09 and 0.03 kcal mol^{-1} from our two HF calculations and 0.32 or 0.46 kcal mol^{-1} for our MP2

Table 4. 6–31G* energies ($E°$) of **1a** with zero point vibration (ZPV) and thermal energy (ThE) corrections (hartree) for Φ_{min}, $\Phi = 0.0°$ and $\Phi = 90°$ and relative energies (kcal mol^{-1}) based on Φ_{min} in comparison with experimental determinations

Method	Φ(°)	$E°$	$E°$ +ZPV	$E°$ +ThE	$\Delta E°$	ΔE ZPV	ΔE ThE	Exp. (90°)	Method	Year
HF	21.76	−307.58519	−307.44210	−307.43577	—	—	—	2.2	Thermodynamic	1946[a]
HF	0.0	−307.58505	−307.44205	−307.43654	0.088	0.031	−0.483	1.78	Raman spectroscopy	1975[b]
HF	90.0	−307.58087	−307.43818	−307.43258	2.713	2.460	2.002	3.27	Fluorescence	1980[c]
B3LYP	0.0	−309.64796	−309.51437	−309.50844	—	—	—	3.06	Fluorescence + Raman	1982[d]
B3LYP	90.0	−309.64123	−309.50794	−309.50191	4.223	4.037	4.010	3.29	Microwave	1988[e]
MP2	28.55	−308.59324	−308.45938	−308.45246	—	—	—			
MP2	0.0	−308.59274	−308.45931	−308.45311	0.316	0.044	−0.408			
MP2	90.0	−308.58908	−308.45535	−308.44916	2.614	2.529	2.071			

[a] Pitzer KS, Guttman L, Westrum EE Jr. *J. Am. Chem, Soc.* 1946; **68**: 2209.
[b] Carreira LA, Towns TG. *J. Chem. Phys.* 1975; **63**: 5283.
[c] Hollas JM, Ridley T. *Chem. Phys. Lett.* 1980; **75**: 94.
[d] Hollas JM, Musa H, Ridley T, Turner PH, Weisenberger KH, Fawcett V. *J. Mol. Spectrosc.* 1982; **94**: 437.
[e] Camiati W, Vogelsanger B, Bauder A. *J. Mol. Spectrosc.* 1988; **128**: 484.

optimizations with both basis sets. Tsuzuki *et al.*[74] found a corresponding HF/6–31G* value of 0.04 kcal mol^{-1} and an MP2/6–31G* value of 0.141 kcal mol^{-1}, which is reduced to 0.109 and 0.100 kcal mol^{-1} from their MP3 and MP4 calculations. The barrier towards $\Phi = 0°$ is naturally 0.0 kcal mol^{-1} in all cases where this is the calculated minimum torsional angle (STO-3G,[72] 6–31G[78] and our B3LYP calculations). Interestingly, our HF/6–31G* value decreases on inclusion of the ZPE correction to 0.031 kcal mol^{-1}, but increases with thermal correction to 0.483 kcal mol^{-1}.

The total energies in Tables 3–6 show clearly that for B3LYP calculations the quantum chemical variation principle which considers the total energy as an indicator of the quality of the applied basis set/method combination is not valid.

*2-Methylstyrene (***2a**). The potential energy curve of **2a** as a function of Φ is shown graphically in Fig. 5 for HF and B3LYP 6–31G* optimizations. In this asymmetrically substituted molecule the periodicity is extended to 180°. This angle represents a *trans* orientation of the vinyl substituent to the *o*-methyl group. The peculiarities of the torsional behaviour are shown more clearly in the DFT plot. The global minimum is found for 154.4° (corresponding to 25.6° in **1a**) for B3LYP and 142.1° (37.9°) in the HF calculation (STO-3G yields 152.7°). A second mimimum is found for $\Phi = 0.0°$ in both calculations, which is fairly high in energy with 3.22 kcal mol^{-1} for B3LYP and 4.82 kcal mol^{-1} for HF calculations. A third minimum is seen at $\Phi = 60°$ in the B3LYP curve where the HF plot shows only a shoulder. The torsional maximum is found with 3.87 kcal mol^{-1} around $\Phi = 30°$ and 4.89 kcal mol^{-1} around $\Phi = 15°$ from B3LYP and HF, respectively. A lower maximum is observed at $\Phi = 180°$ of 0.19 kcal mol^{-1} for B3LYP and 0.77 kcal mol^{-1} for HF optimization, comparable to the lower energy barrier of **1a**. Numerical data are presented in Table 5 with the other vinyl-substituted systems **3a**–**5a**.

*2,6-Dimethylstyrene (***3a**). Figure 6 shows the plot of the potential energy curves of **3a** for HF and B3LYP 6–31G* optimizations. Now both graphs indicate different behaviour in the periodicity of 90°. The HF calculation gives a broad mimimum around $\Phi = 90°$ (with an optimized value of 87.9°) and a single maximum of 3.70 kcal mol^{-1} at $\Phi = 0°$. In contrast, the B3LYP calculation shows two minima, a global one at $\Phi = 64.0°$ (STO-3G yields 56.4°) and a shallow one at $\Phi = 0°$ of 1.01 kcal mol^{-1}. Maxima are found of 0.18 kcal mol^{-1} at $\Phi = 90°$ and 1.06 kcal mol^{-1} around $\Phi = 20°$.

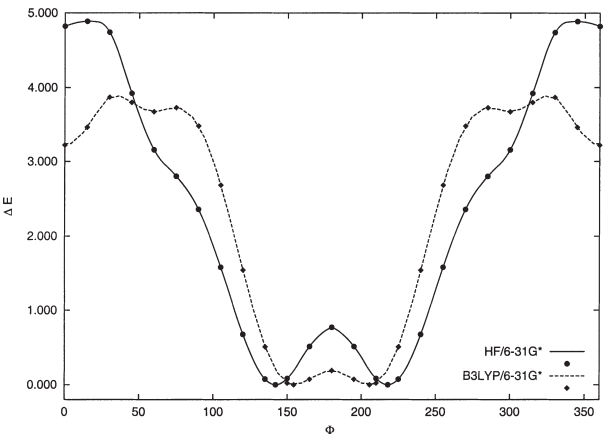

Figure 5. Potential energies (kcal mol^{-1}) of 2-methylstyrene (**2a**) as a function of the torsional angle Φ from HF/6–31G* and B3LYP/6–31G* optimizations for each Φ

Table 5. HF/6–31G* and B3LYP/6–31G* optimized potential energies ΔE (kcal mol^{-1}) of vinyl-substituted benzenoids **2a**–**5a** as a function of the torsional angle Φ

	2-Methylstyrene (**2a**)		2,6-Dimethylstyrene (**3a**)		2-Vinylnaphthalene (**4a**)	1-Vinylnaphthalene (**5a**)
Angle Φ(°)	ΔE HF/6–31G*	ΔE B3LYP/6–31G*	ΔE HF/6–31G*	ΔE B3LYP/6–31G*	ΔE HF/6–31G*	ΔE HF/6–31G*
0	4.822	3.219	3.698	1.014	0.000	2.075
15	4.887	3.462	3.558	1.064	0.068	1.562
30	4.742	3.870	2.896	1.004	0.432	0.556
45	3.922	3.799	1.508	0.442	1.273	0.008
60	3.158	3.675	0.384	0.020	2.372	0.299
75	2.803	3.729	0.032	0.081	3.216	1.091
90	2.360	3.479	0.000	0.183	3.392	1.830
105	1.581	2.686	0.032	0.081	2.836	2.216
120	0.676	1.541			1.882	2.445
135	0.075	0.508			1.098	3.305
150	0.084	0.023			0.904	5.428
165	0.514	0.073			1.171	7.833
180	0.769	0.189			1.359	8.930
Φ_{min}(°)	142.11	154.39	87.90	64.02	0.00	47.00
E_{min} (hatree)	−349.62009	−348.96365	−385.65175	−388.27514	−460.23816	−460.23388

2-Vinylnaphthalene (**4a**) and 1-vinylnaphthalene (**5a**). For these systems only HF/6–31G* optimizations were performed with the numerical data shown in Table 5. Both potential energy curves are presented in Fig. 7.

The periodicity of both asymmetrical systems is again 180°. For $\Phi = 0°$ the vinyl substituent points towards the ring proton H-3 in **4a** and towards H-2 in **5a**. For **4a** two minima are observed, a global one at $\Phi = 0°$ and a higher one at $\Phi = 150°$ of 0.90 kcal mol^{-1}. Maxima are located at $\Phi = 90°$ of 3.39 kcal mol^{-1} and at $\Phi = 180°$ of 1.36 kcal mol^{-1}.

The 1-vinyl substituent in **5a** has a global minimum at $\Phi = 47.0°$ and a small maximum at $\Phi = 0°$ of 2.08 kcal mol^{-1}. A larger maximum is found for $\Phi =$ 180° of 8.93 kcal mol^{-1} which is due to steric interference with the *peri*-hydrogen H-8 of naphthalene in the planar orientation of the vinyl substituent pointing towards this H-8. A shoulder is seen at $\Phi = 120°$.

Isopropenylbenzene (1b)

The numbering of **1b** is shown in Scheme 3. Optimizations are performed with imposed planarity of the phenyl ring with its hydrogens and for the substituent carbons C-15, C-16 with H-17 ($= H_a$) and H-18 ($= H_b$) and C-17 for each torsion Φ in steps of 15°. The rotational angle τ of the methyl group was optimized with the other parameters for each angle Φ.

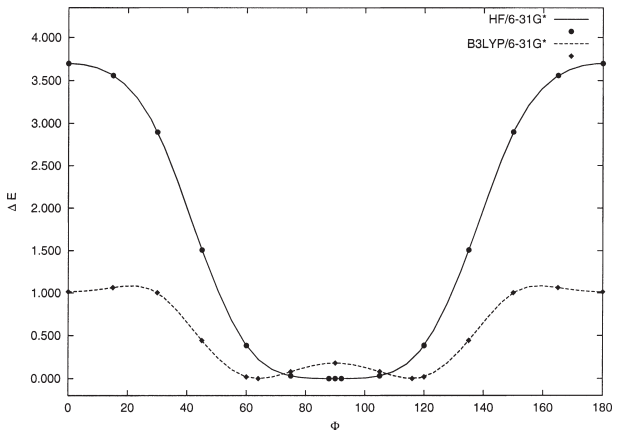

Figure 6. Potential energies (kcal mol^{-1}) of 2,6-dimethylstyrene (**3a**) as a function of the torsional angle Φ from HF/6–31G* and B3LYP/6–31G* optimizations for each Φ

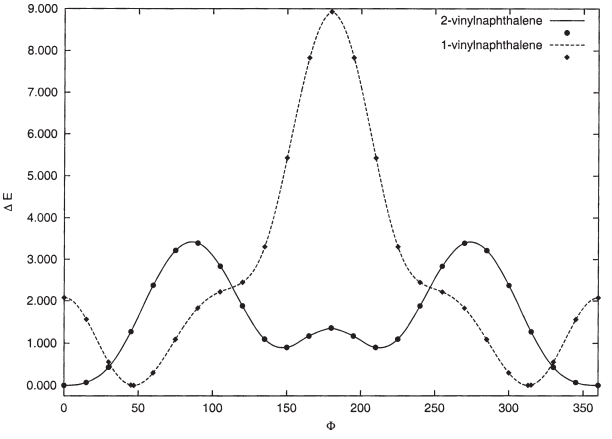

Figure 7. Potential energies (kcal mol^{-1}) of 2-vinylnaphthalene (**4a**) and 1-vinylnaphthalene (**5a**) as a function of the torsional angle Φ from HF/6–31G* optimizations for each Φ

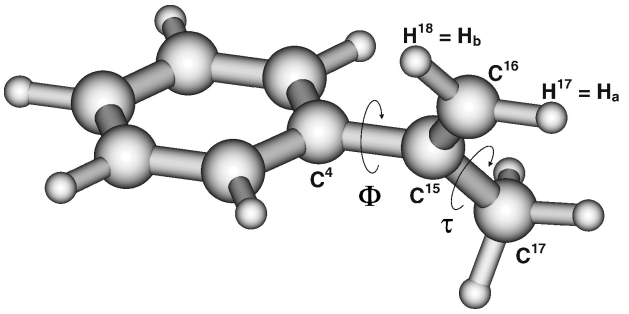

Scheme 3. Indication of torsional angle Φ and CH_3 rotation angle τ in isopropenyl benzene (**1b**)

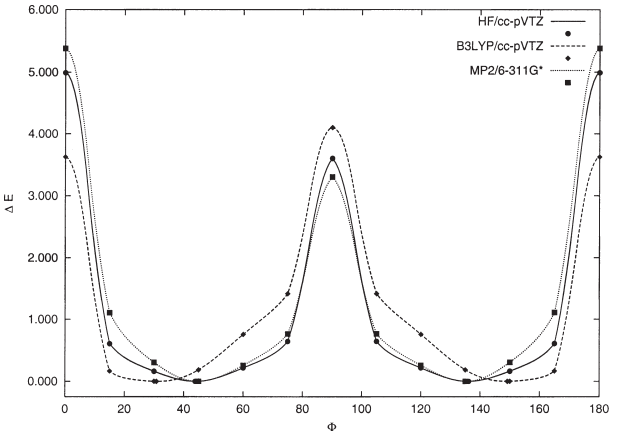

Figure 8. Potential energies (kcal mol^{-1}) of isopropenylbenzene (**1b**) as a function of the torsional angle Φ from HF/cc-pVTZ, B3LYP/cc-pVTZ and MP2/6–311G* optimizations

The potential energy plot for the three methods with triple zeta basis sets in Fig. 8 shows a periodicity of 90°. All six calculations listed in Table 6 show a similar behaviour. As expected, the torsional Φ_{min} angles are larger than in **1a**. Φ_{min} is around 44° from HF calculations, around 29° for the two B3LYP optimizations and 41.9 and 44.9° for the two MP2 calculations. Maxima of total energy are found at $\Phi = 0$ and 90°. The HF calculation yields a larger barrier at $\Phi = 0°$ of 5.20 kcal mol^{-1} for 6–31G* and 4.99 kcal mol^{-1} for cc-pVTZ. The MP2 optimizations lead for the same angle to 5.25 kcal mol^{-1} with 6–31G* and 5.38 kcal mol^{-1} for 6–311G*. The 90° barrier is smaller, 3.56 or 3.50 kcal mol^{-1} for HF and 3.77 and 3.20 kcal mol^{-1} for MP2 calculations.

The two B3LYP optimizations indicate an opposite behaviour. The 0° barrier is the smaller one at around 3.8 kcal mol^{-1} and the 90° barrier is now the larger one at 4.59 and 4.10 kcal mol^{-1}, respectively.

The optimizations in Table 6 yielded different methyl group orientations for each angle Φ. To eliminate this effect, we performed separate rotations (τ) of the methyl group from one CH bond projected on to the C=CH_2 plane in steps of $\tau = 15°$ starting from $\tau = 0°$. This periodicity is 60°. For $\tau = 60°$ the two CH bonds bisect the vinylic plane, which is the most favourable methyl group conformation with a relative energy of 0.0 kcal mol^{-1}. The resulting energetic effect in the case of $\Phi = 0°$ and $\tau = 0°$ is surprisingly large at 4.13 kcal mol^{-1}. For $\Phi = 45°$ the maximum effect of 2.07 kcal mol^{-1} is smaller and shows a periodicity of 120°. The maximum effect for $\Phi = 90°$ is 2.55 kcal mol^{-1}. Numerical values are presented in Table 7.

Calculations of chemical shifts of vinyl protons

Our GIAO MO-calculated ^{1}H NMR chemical shifts for the vinylic protons (H_a, H_b and H_c) for three representative torsional angles (Φ_{min}, $\Phi = 0°$ and $\Phi = 90°$) in the applied methods for the optimized geometries in Tables 3, 5 and 6 are presented in Table 8. The originally obtained shielding values (which refer to a naked proton as zero point) were converted to the listed δ-values by means of calculated TMS shielding values (which are included in the heading of Table 8) for each method–basis set combination based on TMS geometries optimized within the same procedure.

Table 6. Basis set and method dependence of optimized potential energies ΔE (kcal mol^{-1}) for isopropenylbenzene (**1b**) as a function of the torsional angle Φ[a]

Angle Φ(°)	ΔE HF/ 6–31G*	ΔE HF/ cc-pVTZ	ΔE B3LYP/ 6–31G*	ΔE B3LYP/ cc-pVTZ	ΔE MP2/ 6–31G*	ΔE MP2/ 6–311G*
0	5.195	4.990	3.820	3.622	5.248	5.381
15	0.770	0.610	0.135	0.168	0.939	1.106
30	0.212	0.164	0.002	0.001	0.217	0.308
45	0.001	0.001	0.279	0.187	0.014	0.0001
60	0.242	0.217	0.982	0.757	0.421	0.260
75	0.729	0.644	1.771	1.412	1.050	0.764
90	3.561	3.598	4.592	4.101	3.767	3.299
Φ_{min} (°)	44.29	43.87	28.45	30.82	41.87	44.89
E_{min} (hatree)	−346.62137	−346.73725	−348.96424	−349.08947	−347.76418	−347.88050

[a] Ref. 72: HF/STO-3G, $\Phi_{min} = 34.1°$, $E_{min} = -342.41635$ hartree, $\Delta E_{0°} = 0.81$ kcal mol^{-1}, $\Delta E_{90°} = 1.74$ kcal mol^{-1}.

Table 7. HF/6–31G* calculated torsional potentials ΔE (kcal mol^{-1}) for isopropenylbenzene (**1b**) with the methyl group fixed in the alkene plane and five selected rotations τ of the methyl group relative to this plane

Angle Φ (°)	ΔE Φ = variable	ΔE $\Phi = 0°$ fixed	ΔE $\Phi = 45°$ fixed	ΔE $\Phi = 90°$ fixed	Rotation angle τ (°)
0	3.098	4.126			0
		3.559			15
		2.144			30
		0.649			45
		0.000			60
15	2.251				
30	0.703				
45	0.000		2.072		0
			1.926		15
			1.278		30
			0.482		45
			0.000		60
			0.141		75
			0.828		90
			1.628		105
			2.072		120
60	0.401				
75	1.133				
90	1.464			2.553	0
				2.186	15
				1.289	30
				0.380	45
				0.000	60
Φ_{min} (°)	44.29				
E_{min} (hatree)	−346.62137				

The chemical shifts in Table 8 vary over a considerable range depending on the method and basis set, especially for Φ_{min}, which delivers in each case a different minimum torsional angle. For H_a and H_b of **1a** the calculated shifts span a range from 0.8 to 1.1 ppm depending on Φ and the method–basis set combination (see Fig. 9). For H_c, which is not considered explicitly, this range is even larger. However, for the splitting of calculated geminal proton signals the variation with basis sets is only 0.15 ppm at $\Phi = 0°$ and 0.06 ppm at $\Phi = 90°$, i.e. this splitting can be predicted with similar precision in each of the applied procedures. The largest chemical shifts and splittings result from B3LYP/cc-pVTZ calculations.

Estimation of effective torsional angles Φ_{eff}

All presented calculations of chemical shifts and splittings are based on a frozen geometry and $E°$ energies of isolated molecules. However, the experimental chemical shifts in Tables 1 and 2 refer to flexible dynamic molecular systems in $CDCl_3$ solutions at a measuring temperature of about 300 K. Therefore, the question remains: are the potential energy curve and Φ_{min} sufficient for comparison?

This can be tackled empirically by use of the splitting curves which we have at hand separately for each calculation. Starting from the experimental splitting value on the *y*-axis, we take from the splitting curve the corresponding apparent effective Φ_{eff} value with results presented in Table 8 in comparison with Φ_{min} values. The largest deviations are found for DFT calculations of **1a** where Φ_{eff} values of 16 and 24° are in contrast to the calculated Φ_{min} angle of 0°. The derived Φ_{eff} angles are nearly independent of the methods and basis sets. For **1a** this range is from 16° to 25° in comparison with optimized Φ_{min} values between 0 and 31°.

Chemical shifts calculated for isopropenylbenzene (**1b**) are given in Table 9. These also vary considerably by more than 1 ppm. Derived Φ_{eff} angles for **1b** between 25 and 30° are all smaller than the calculated Φ_{min} angles, between 28.5° and 44.9°.

Examples of the angular dependence of calculated shieldings of **1b** are shown in Fig. 10.

Calculated splitting of geminal proton signals

Vinyl systems

The influence of basis sets and methods on the calculated splitting of **1a** is shown numerically in Table 10 and graphically for three examples in Fig. 11.

We will concentrate in the following discussions on the HF/6–31G* calculations because these calculations are available for all molecules **1a**–**5a** and **1b**. The strong dependence of splittings of **1a** on rotation angle Φ is clearly seen in Table 10. Up to an angle Φ of about 50° the splittings are negative from −0.60 ppm up to a maximum positive splitting of 0.21 ppm for $\Phi = 90°$.

Table 8. GIAO MO 6–31G* calculated ^{1}H chemical shifts (ppm) of vinyl derivatives which are converted from shielding values by use of the following geometry optimized TMS values: HF/6–31G* = 32.9033 ppm; B3LYP/6–31G* = 32.9035 ppm; MP2/6–31G* = 32.0281 ppm; HF/cc-pVTZ = 32.2531 ppm; B3LYP/cc-pVTZ = 32.0320 ppm; MP2/6–311G* = 32.6068 ppm

Compound	Method	Φ (°)	δH_a	δH_b	δH_c	$\Delta\delta(H_a - H_b)$	Φ_{eff} (°)
1a	Experiment	?	5.16	5.66	—	−0.50	
min	HF/6–31G*	21.76	5.441	5.749	6.863	−0.437	17
min	B3LYP/6–31G*	0.0	5.154	5.748	6.351	−0.594	16
min	MP2/6–31G*	28.55	4.896	5.290	6.358	−0.394	23
min	HF/cc-pVTZ	16.37	5.433	6.031	6.931	−0.598	23
min	B3LYP/cc-pVTZ	0.0	5.678	6.422	7.167	−0.744	24
min	MP2/6–311G*	31.42	5.609	5.994	7.200	−0.384	25
1a	HF/6–31G*	0.0	5.386	5.986	6.604	−0.600	
	B3LYP/6–31G*	0.0	5.159	5.752	6.347	−0.593	
	MP2/6–31G*	0.0	4.833	5.523	6.095	−0.690	
	HF/cc-pVTZ	0.0	5.426	6.031	6.842	−0.696	
	B3LYP/cc-pVTZ	0.0	5.678	6.422	7.167	−0.744	
	MP2/6–311G*	0.0	5.554	6.280	6.881	−0.726	
1a	HF/6–31G*	90.0	5.592	5.385	5.385	0.207	
	B3LYP/6–31G*	90.0	5.386	5.158	7.117	0.228	
	MP2/6–31G*	90.0	5.073	4.872	6.665	0.200	
	HF/cc-pVTZ	90.0	5.646	5.424	7.339	0.221	
	B3LYP/cc-pVTZ	90.0	5.917	5.655	7.801	0.262	
	MP2/6–311G*	90.0	5.805	5.592	7.491	0.213	
2a	Experiment	?	5.277	5.621	6.945	−0.344	
min	HF/6–31G*	142.11	5.495	5.664	6.980	−0.170	154
min	B3LYP/6–31G*	154.39	5.220	5.558	6.828	−0.338	147
	HF/6–31G*	0.0	5.426	5.697	6.672	−0.272	
	B3LYP/6–31G*	0.0	5.245	5.491	6.546	−0.246	
	HF/6–31G*	90.0	5.609	5.339	7.028	0.270	
	B3LYP/6–31G*	90.0	5.415	5.121	7.026	0.291	
	HF/6–31G*	180.0	5.478	5.960	6.960	−0.534	
	B3LYP/6–31G*	180.0	5.193	5.709	6.766	−0.515	
3a	Experiment	?	5.526	5.248	6.691	0.278	
min	HF/6–31G*	87.90	5.616	5.291	6.919	0.324	69
min	B3LYP/6–31G*	64.01	5.468	5.247	6.833	0.221	70
	HF/6–31G*	0.0	5.462	5.654	7.025	−0.192	
	B3LYP/6–31G*	0.0	5.278	5.436	6.964	−0.158	
	HF/6–31G*	90.0	5.616	5.290	6.920	0.326	
	B3LYP/6–31G*	90.0	5.420	5.073	6.952	0.348	
4a	Experiment	?	5.25	5.75	6.80	−0.50	
min	HF/6–31G*	0.0	5.465	6.039	6.836	−0.574	150; 14
	HF/6–31G*	90.0	5.688	5.494	7.298	0.194	
	HF/6–31G*	180.0	5.501	6.232	6.701	−0.717	
5a	Experiment	?	5.36	5.65	—	−0.29	
min	HF/6–31G*	47.00	5.671	5.780	7.507	−0.109	151; 37
	HF/6–31G*	0.0	5.643	6.234	7.529	−0.592	
	HF/6–31G*	90.0	5.858	5.534	7.308	0.323	
	HF/6–31G*	180.0	5.506	6.194	6.781	−0.688	

The torsional dependence of calculated splittings of molecules **2a**–**5a** are presented in Table 11. Asymmetrically substituted **2a** shows a periodicity in 180°. Its largest negative splitting is −0.53 ppm at 180° for the sterically unfavourable orientation of the vinyl group towards the *o*-methyl substituent. The second energetic maximum at Φ = 0° shows a splitting of −0.272 ppm and the maximum positive splitting of 0.29 ppm occurs at Φ = 75°. Surprisingly, the splitting at Φ = 90° is lower, 0.27 ppm.

For the symmetrically substituted **3a** the lowest splitting is −0.19 ppm for the sterically unfavourable zero angle and the maximum value at Φ = 90° of 0.33 ppm is larger than the maximum **1a** value. This indicates an influence of the two *o*-methyl substituents.

Asymmetric vinylnaphthalenes **4a** and **5a** again have a periodicity of 180°. The largest negative splitting is −0.57 ppm for unfavourable Φ = 0° and a lower splitting of −0.27 ppm at Φ = 180°. The maximum positive value of 0.21 ppm occurs at Φ = 75°, not at 90°.

In **5a**, both planar orientations at Φ = 0 and 180° lead to similar large splittings of −0.59 and −0.69 ppm. The largest positive splitting is calculated as 0.32 ppm for Φ = 90°. This shows a larger influence of both benzene units of naphthalene in the 1-position relative to the 2-position in **4a**. This effect is much larger for the

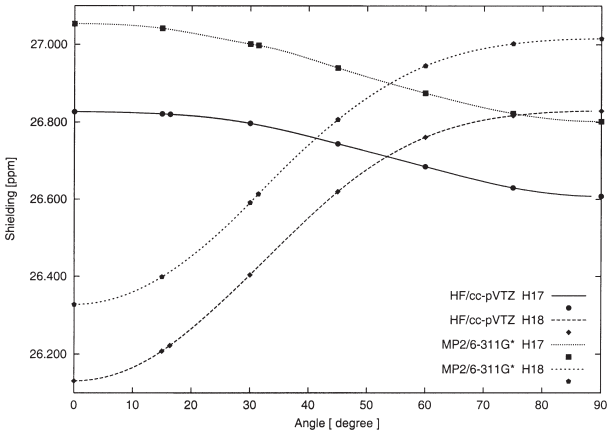

Figure 9. Shieldings (ppm) of H_a and H_b protons of styrene (**1a**) from HF/cc-pVTZ and MP2/6–311G* GIAO calculations (in Figs 9, 10, 13 and 14 H_a is denoted as H17 and H_b as H18)

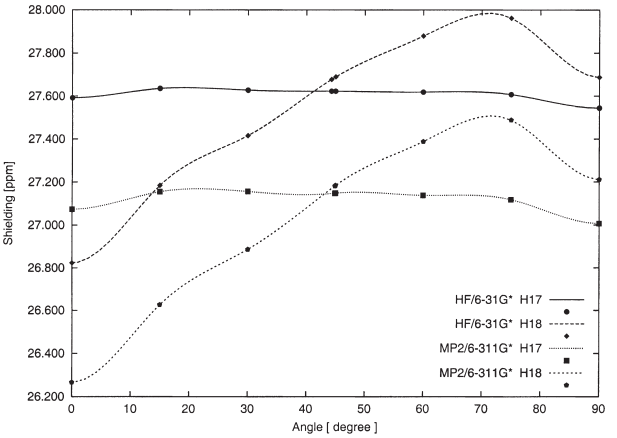

Figure 10. Shieldings (ppm) of H_a and H_b protons of isopropenylbenzene (**1b**) from HF/6–31G* and MP2/6–311G* GIAO calculations

calculated splitting of 9-vinylanthracene (**8a**) of 0.48 ppm at $\Phi = 90°$. The experimental value of 0.34 ppm indicates a smaller torsional angle.

Isopropenyl benzene (1b)

The results for the angular dependence of all six calculations of splitting for **1b** are presented in Table 12. An accidental perfect agreement of splitting with the experiment for **1b** shows a B3LYP/cc-pVTZ value of −0.282 ppm. The maximum splitting is calculated as 0.354 ppm for $\Phi = 75°$ and not as expected for $\Phi = 90°$. The numerical values, which range between −0.77 and 0.14 ppm for $\Phi = 0$ and 90° are all smaller than the corresponding values of **1a**.

Now we may study quantitatively how much the methyl substituent in **1b** affects the geminal splitting in relation to that of **1a** for each angle Φ just by taking differences of the corresponding values in Tables 10 and 12. The differences vary irregularly in the range 0.17–0.064 ppm.

The graphical representation of splitting in Fig. 12 shows an irregular behaviour which is due to the combined variation of both the torsion Φ and the methyl group rotation τ. Therefore, we fixed one CH orientation in the olefinic plane for all torsions Φ, which now leads to a smooth curve for splittings, as shown in Fig. 13. The effect of the additional methyl group rotation τ at $\Phi = 0°$ is shown in Fig. 14.

The resulting numerical values for different Φ and τ values are given in Table 13.

The difference in the respective splittings in Tables 10 and 13 yield for fixed CH bonds at unfavourable $\tau = 0°$ a smooth decrease from 0.164 ppm at $\Phi = 0°$ to 0.064 ppm at $\Phi = 90°$. For the favourable methyl orientation with $\tau = 60°$ this is order reversed: 0.065 ppm at $\Phi = 0°$ and 0.176 ppm at $\Phi = 90°$. It is interesting that the alkyl group increments for the influence on *cis* and *trans* vinyl hydrogens in the tabulation of Pretsch *et al.*[79] yield a difference of 0.06 ppm.

Table 9. GIAO MO calculated chemical shifts (ppm) of **1b** from shielding with TMS values presented in the heading of Table 8

Method/basis set	Φ (°)	δH_a	δH_a	$\Delta\delta$ ($H_a - H_b$)	Φ_{eff} (°)
Experiment	?	5.079	5.361	−0.282	
HF/6–31G*	44.29	5.281	5.226	0.035	25
B3LYP/6–31G*	28.45	5.048	5.302	−0.254	27
MP2/6–31G*	41.87	4.741	4.759	−0.018	
HF/cc-pVTZ	43.87	5.284	5.282	0.002	30
B3LYP/cc-pVTZ	30.82	5.568	5.650	−0.282	30
MP2/6–311G*	44.89	5.459	5.426	0.034	
HF/6–31G*	0.0	5.312	6.081	−0.769	
B3LYP/6–31G*	0.0	5.097	5.875	−0.778	
MP2/6–31G*	0.0	4.779	5.620	−0.841	
HF/cc-pVTZ	0.0	5.312	6.081	−0.769	
B3LYP/6–31G*	0.0	5.097	5.875	−0.778	
MP2/6–31G*	0.0	4.779	5.620	−0.841	
HF/6–31G*	90.0	5.359	5.216	0.143	
B3LYP/6–31G*	90.0	5.167	5.015	0.152	
MP2/6–31G*	90.0	4.843	4.694	0.149	
HF/cc-pVTZ	90.0	5.395	5.198	0.197	
B3LYP/cc-pVTZ	90.0	5.694	5.469	0.225	
MP2/6–311G*	90.0	5.600	5.396	0.204	
HF/6–31G*	75.0	5.296	4.942	0.354	
B3LYP/6–31G*	75.0	5.098	4.737	0.361	
MP2/6–31G*	75.0	4.763	4.413	0.350	
HF/cc-pVTZ	75.0	5.325	4.959	0.366	
B3LYP/cc-pVTZ	75.0	5.616	5.333	0.394	
MP2/6–311G*	75.0	5.489	5.118	0.370	

APUDI model calculations

The principle of our APUDI model[51] is shown in Scheme 4. Perpendicular above and below each benzenoid carbon atom is placed a dimagnetic point dipole at a distance $p = 0.7$ Å and the distances from these points to the considered proton H_j are summed for $2n$ atomic

Table 10. Basis set, method and angular dependence of GIAO MO calculated splitting $\Delta\delta$ ($H_a - H_b$) (ppm) of geminal vinyl group protons of styrene (**1a**)

Angle Φ (°)	HF/6–31G*	HF/cc-pVTZ	B3LYP/6–31G*	B3LYP/cc-pVTZ	MP2/6–31G*	MP2/6–311G*
0	−0.600	−0.696	−0.593	−0.744	−0.690	−0.726
15	−0.520	−0.614	−0.515	−0.650	−0.603	−0.642
30	−0.308	−0.393	−0.297	−0.393	−0.366	−0.410
45	−0.064	−0.125	−0.031	−0.085	−0.092	0.133
60	0.102	0.077	0.137	0.125	0.094	0.071
75	0.185	0.188	0.211	0.231	0.179	0.180
90	0.207	0.221	0.228	0.262	0.200	0.213
Φ_{min} (°)	21.76	16.37	0.00	0.00	28.855	31.42
$\Delta\delta_{min}$	−0.437	−0.598	−0.594	−0.744	−0.394	−0.384

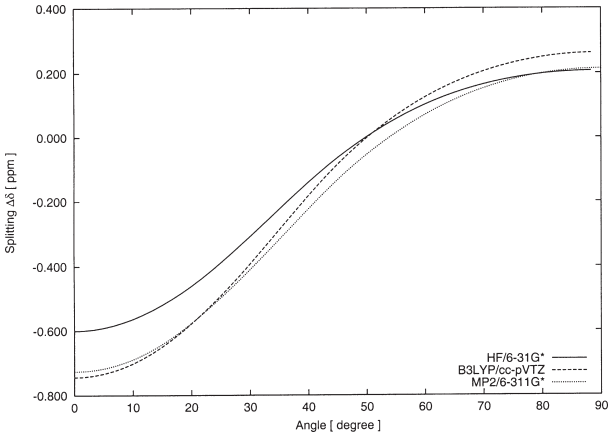

Figure 11. Splittings (ppm) of geminal protons ($\Delta\delta = \delta H_a - \delta H_b$) of styrene (**1a**) from HF/6–31G*, B3LYP/cc-pVTZ and MP2/6–311G* GIAO calculations

magnetic dipoles via equivalent Eqn (1) or (2), leading to a purely geometric factor denoted GF_j in Eqn (3):

$$\Delta\delta_j[\text{ppm}] = EAS \cdot \sum_{i=1}^{2n} \frac{1 - 3\cos^2\Phi_{ij}}{3R_{ij}^3} \tag{1}$$

$$\Delta\delta_j[\text{ppm}] = EAS \cdot \sum_{i=1}^{2n} \frac{d_{ij}^2 - 2p^2}{3\left(d_{ij}^2 + p^2\right)^{5/2}} \tag{2}$$

$$\Delta\delta_j[\text{ppm}] = EAS \cdot GF_j \tag{3}$$

The ring current contribution to the chemical shift of an aromatic proton ($\Delta\delta_j$) is obtained via Eqn (3) by multiplication of GF_j with a constant effective atomic susceptibility (EAS) which was determined empirically

Table 11. Angular dependence HF/6–31G* and B3LYP/6–31G* GIAO MO calculated splittings $\Delta\delta$ ($H_a - H_b$) (ppm) of geminal vinyl group protons of vinyl-substituted benzenoids[a]

	2-Methylstyrene (**2a**)		2,6-Dimethylstyrene (**3a**)		2-Vinylnaphthalene (**4a**)	1-Vinylnaphthalene (**5a**)
Angle Φ (°)	HF/6–31G*	B3LYP/6–31G*	HF/6–31G*	B3LYP/6–31G*	HF/6–31G*	HF/6–31G*
0	−0.272	−0.246	−0.192	−0.158	−0.574	−0.592
15	−0.220	−0.199	−0.155	−0.128	−0.489	−0.529
30	−0.097	−0.094	−0.065	−0.072	−0.265	−0.355
45	0.063	0.020	0.058	0.007	−0.015	−0.137
60	0.221	0.193	0.212	0.180	0.150	0.055
75	0.286	0.291	0.302	0.306	0.208	0.202
90	0.270	0.294	0.326	0.348	0.194	0.323
105	0.206	0.232			0.129	0.412
120	0.096	0.129			0.009	0.390
135	−0.071	−0.044			−0.188	0.135
150	−0.282	−0.276			−0.559	−0.283
165	−0.465	−0.453			−0.348	−0.583
180	−0.534	−0.515			−0.268	−0.688
Φ_{min} (°)	142.11	154.39	87.90	64.02	0.00	47.00
$\Delta\delta_{min}$	−0.1696	−0.3384	0.3243	0.2211	−0.5740	−0.1086

[a] HF/6–31G* optimization for **8a** with fixed $\Phi = 90°$ leads to $\Delta\delta = 0.476$ ppm at $E = -612.87235$ hartree.

Table 12. Basis set, method and angular dependence of GIAO MO calculated splitting $\Delta\delta$ ($H_a - H_b$) (ppm) of geminal vinyl group protons of isopropenylbenzene[a] (**1b**)

Angle Φ (°)	HF/6–31G*	HF/cc-pVTZ	B3LYP/6–31G*	B3LYP/cc-pVTZ	MP2/6–31G*	MP2/6–311G*
0	−0.769	−0.858	−0.778	−0.964	−0.841	−0.807
15	−0.451	−0.541	−0.480	−0.629	−0.525	−0.529
30	−0.212	−0.280	−0.222	−0.302	−0.266	−0.270
45	0.067	0.021	0.082	0.051	0.042	0.035
60	0.280	0.245	0.275	0.287	0.252	0.251
75	0.354	0.366	0.361	0.394	0.350	0.370
90	0.143	0.197	0.152	0.225	0.149	0.204
Φ_{min} (°)	44.29	43.87	28.45	30.82	41.87	44.89
$\Delta\delta_{min}$	0.055	0.002	−0.254	−0.282	−0.0181	0.0335

[a] Ref. 72: HF/STO-3G $\Phi_{min} = 34.1°$.

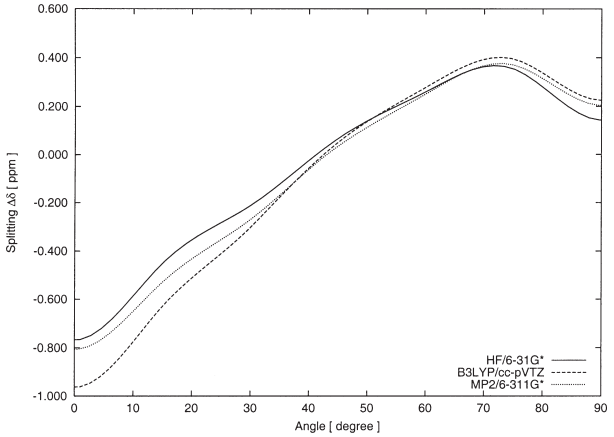

Figure 12. Splittings (ppm) of geminal protons ($\Delta\delta = \delta H_a - \delta H_b$) of **1b** from HF/6–31G*, B3LYP/cc-pVTZ and MP2/6–311G* GIAO calculations

as a function p from the slope of linear regression between the experimental chemical shifts of ring protons of 14 benzenoids with corresponding GF_j values calculated for standard geometries, which lead to $EAS(0.7) = -14.50 \times 10^{-6}$ Å^{-3} for $p = 0.7$ Å. The statistics surprisingly yielded the smallest standard error and largest correlation coefficient for $p = 0.0$ Å with $EAS(0.0) = -10.67 \times 10^{-6}$ Å^{-3} if two point dipoles are placed at the position of carbon nucleus C_i. For applications of APUDI calculations shown in Table 14 we used both selections.

Symmetry reduces the number of atomic point dipole positions which have to be evaluated: for benzene only four points are necessary, leading for $p = 0.7$ Å to a GF of 0.1586 Å^{-3}, which yields a ring current contribution of 1.983 ppm and a chemical shift of 7.143 ppm.

In Fig. 15 is shown the torsional dependence of ring current contributions for H_a and H_b protons for the π-electron models of Johnson-Bovey[46,47] (a) and of Haigh-Mallion[50] (b) compared with APUDI GF values (c). The numerical values of both π-models are too small.

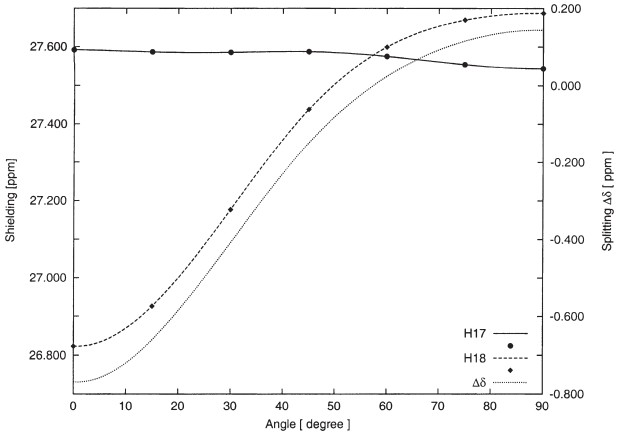

Figure 13. Φ dependence of shieldings and splittings ($\Delta\delta$) of H_a and H_b protons (ppm) of **1b** with the CH_3 group fixed at $\tau = 0°$ from HF/6–31G* calculations

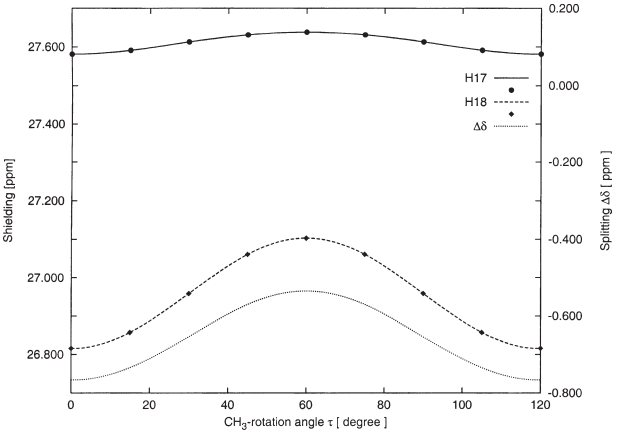

Figure 14. Influence of CH_3 group rotation of **1b** of shieldings and splittings ($\Delta\delta$) of H_a and H_b protons (ppm) for τ from 0° to 60° at $\Phi = 0°$ from HF/6–31G* calculations

Table 13. HF/6–31G* GIAO MO calculated splitting $\Delta\delta(H_a - H_b)$ (ppm) of geminal vinyl group protons of isopropenylbenzene (**1b**) with fixed methyl group and five selected methyl group rotations τ

Angle Φ (°)	$\Delta\delta$ (ppm)	$\Phi = 0°$ fixed	$\Phi = 45°$ fixed	$\Phi = 90°$ fixed	Rotation angle τ (°)
0	−0.764	−0.766			0
		−0.734			15
		−0.654			30
		−0.570			45
		−0.535			60
15	−0.661				
30	−0.408				
45	−0.150		−0.149		0
			−0.100		15
			−0.013		30
			0.059		45
			0.075		60
60	0.024				
75	0.115				
90	0.143			0.144	0
				0.179	15
				0.264	30
				0.349	45
				0.383	60
Φ_{min} (°)	44.29				
$\Delta\delta_{min}$	0.055				

The APUDI model simulates, owing to its empirically derived *EAS* values, a combination of σ- and π-electron contributions. (This is shown by the better modelling of shielding of crowded hydrogens such as the 4,5-proton signals of phenanthrene.[51])

The angular dependence of APUDI-predicted splittings for **1a** and **1b** are shown in Table 14 for the two *p* values and graphically in Fig. 16. The in-plane values for $\Phi = 0°$ are similar to those of the GIAO calculations in Tables 10 and 12 but the values for $\Phi = 90°$ are definitely too large.

Relevance of ring current effects

In 1965, Musher[80] questioned the Pauling–Pople ring current model of π-electrons in benzene, indicating the importance of neglected σ-electrons by arguing about the additivity of magnetic contributions, which led to controversial discussions.[81] As a consequence, the importance of local σ-contributions in addition to delocalized π-electron contributions was treated in the models of Barfield *et al.*[52] and Blustin[53] and also in advanced calculations by Agarwal *et al.*[82] and Vogler.[57]

The relation of both contributions has been debated quantitatively by coupled Hartree–Fock (CHF) all-electron *ab initio* calculations by Lazzeretti *et al.*,[83] who obtained magnetic shielding contributions close to the HF limit for core, σ- and π-electrons to shieldings of benzene hydrogens in nearly similar ratios.

Recently, Wannere and Schleyer,[84] by application of IGLO B3LYP/6–311+G** calculations, completely rejected the occurrence of π-electron ring currents as a reason for the low-field shift of benzenoid proton signals. However, this conclusion was refuted as being conceptually wrong by Viglione *et al.*,[85] stressing the importance of the interpretative value of the ring current model as being valid and still alive.

Our empirical APUDI model simulates both σ- and π-effects and the GIAO calculations are completely independent of σ- and π-separations. However, both applications model the experimentally observed trends convincingly.

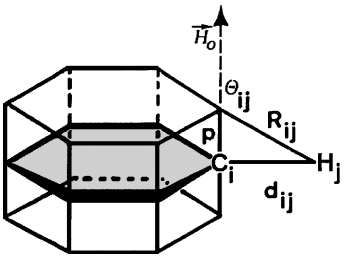

Scheme 4. Definition of parameters used in the APUDI model with Eqns (1)–(3)

CONCLUSION

We showed by use of experimental ^{1}H NMR data in comparison with GIAO calculations of chemical shifts for optimized geometries and APUDI predictions that the splitting of the geminal proton signals of vinyl or isopropenyl substituents on aromatic systems may be used as an indicator of magnetic anisotropies similar as the previously used mesityl substituents. These values indicate a probing of differences of iso-shielding lines. The

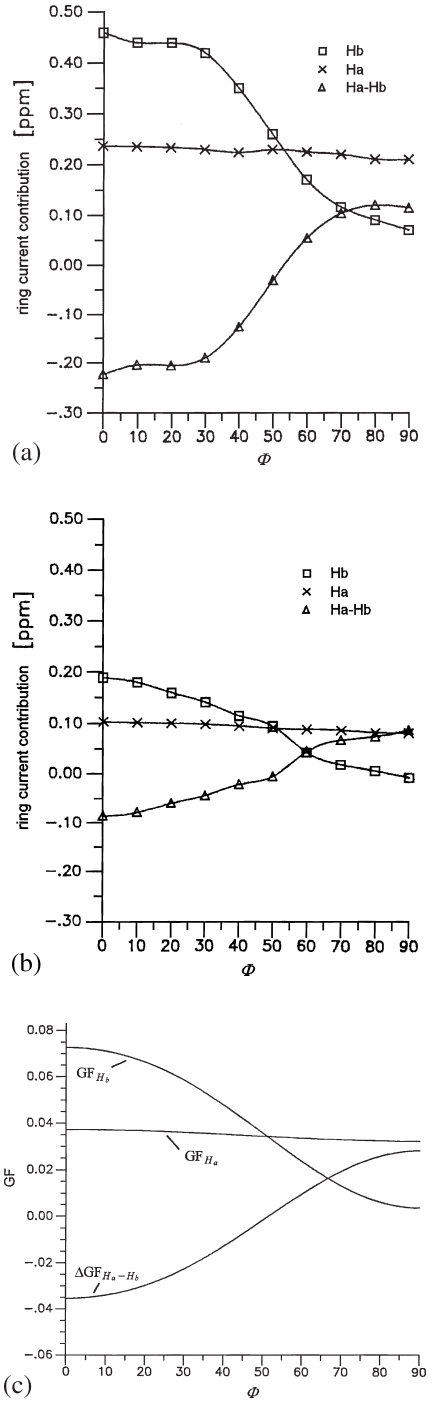

Figure 15. (a) Ring current contribution (ppm) to splitting of geminal protons ($\Delta\delta = \delta H_a - \delta H_b$) of styrene (**1a**) from Johnson–Bovey tables as a function of Φ. (b) Ring current contribution (ppm) to splitting of geminal protons ($\Delta\delta = \delta H_a - \delta H_b$) of styrene (**1a**) from Haigh–Mallion tables as a function of Φ. (c) Geometry factor (*GF*) of the APUDI model as a function of Φ for the splitting of geminal protons ($\Delta\delta = \delta H_a - \delta H_b$) of styrene (**1a**)

numerical values depend critically on the rotational orientation of the considered groups. For nearly perpendicular arrangements for **8a** and **8b** values in the range up to 0.62 ppm are observed.

Table 14. APUDI calculated splitting $\Delta\delta$ ($H_a - H_b$) (ppm) of geminal vinyl group protons of styrene (**1a**) and isopropenylbenzene (**1b**) for STO-3G geometries

Angle	**1a**		**1b**	
Φ (°)	$p = 0.0$ Å	$p = 0.7$ Å	$p = 0.7$ Å	$p = 0.7$ Å
0	−0.523	−0.513	−0.630	−0.609
15	−0.45	−0.49	−0.523	−0.566
30	−0.21	−0.35	−0.256	−0.406
45	0.05	−0.12	0.085	−0.131
60	0.29	0.15	0.331	0.150
75	0.43	0.32	0.501	0.377
90	0.49	0.41	0.587	0.522
Φ_{min}(°)	0.0	0.0	34.1	34.1
$\Delta\delta_{min}$	−0.526	−0.513	−0.147	−0.326

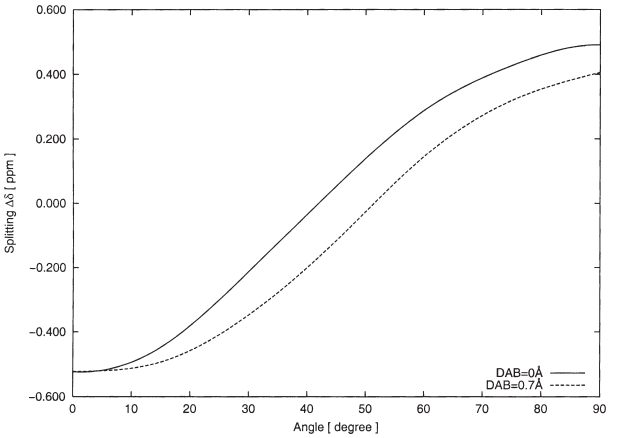

Figure 16. APUDI model calculation as a function of Φ of the splitting (ppm) of geminal protons $\Delta\delta$ for **1a** based on STO-3G geometries for $p = 0.0$ and 0.7 Å

Advantages of the vinyl substituent splitting against the mesityl group splitting are the simpler synthesis, the more precise localization of the geometric positions and the dependence solely on the rotational angle Φ. A disadvantage is that in unaffected positions the vinyl groups are in the low-field range and negative splitting occurs.

REFERENCES

1. Minkin VI, Glukhovtsev MN, Simkin BYa. *Aromaticity and Antiaromaticity: Electronic and Structural Aspects*. Wiley: New York, 1994.
2. Lloyd B. *The Chemistry of Conjugated Cyclic Compounds: To Be or Not to Be Like Benzene?* Wiley: Chicester, 1989.
3. Garratt PJ. *Aromaticity*. Wiley: New York, 1986.
4. Lewis D, Peters D. *Facts and Theories of Aromaticity*. Macmillan: London, 1975.
5. Badger GM. *Aromatic Character and Aromaticity*. Cambridge University Press: Cambridge, 1969.
6. Krygowski TM, Cyrański MK, Czarnocki Z, Häfelinger G, Katritzky AR. *Tetrahedron* 2000; **56**: 1783–1796.
7. Schleyer PvR (guest ed). *Thematic Issue on Aromaticity. Chem. Rev.* 2001; **101**: 1115–1566.

8. Neus J. *Aromatizität: Geschichte und Mathematische Analyse eines fundamentalen chemischen Begriffs*, Schummer J (ed). Hyle Studies No. 2, Karlsruhe, 2002; 1–212.
9. Kekulé FA. *Bull. Soc. Chim. Fr.* 1865; **3**: 98–110; *Ann. Chem. Pharm.* 1866; **137**: 129–196.
10. (a) March J. *Advanced Organic Chemistry: Reactions, Mechanism, and Structure* (3rd edn). Wiley: New York, 1985; chapt. 11; (b) Ingold CK. *Structure and Mechanism in Organic Chemistry* (2nd edn). Cornell University Press: Ithaca, NY, 1969; chapt. VI; (c) Koerner W. *Gazz. Chim. Ital.* 1874; **4**: 437–445.
11. (a) Wheland GW. *J. Am. Chem. Soc.* 1942; **64**: 900–908. (b) Pfeiffer P, Wizinger R. *Liebigs Ann. Chem.* 1928; **461**: 132–154.
12. Armit JW, Robinson R. *J. Chem. Soc.* 1925; **127**: 1604–1618.
13. (a) Hückel E. *Z. Elektrochem.* 1937; **43**: 752–788; (b) Hückel E. *Z. Phys.* 1931; **70**: 204–286; (c) Hückel E. *Z. Phys.* 1931; **72**: 310–337; (d) Hückel E. *Z. Phys.* 1932; **76**: 628–648.
14. Streitwieser A Jr. *Molecular Orbital Theory for Organic Chemists*. Wiley: New York, 1961.
15. Cyrański MK. *Chem. Rev.* 2005; **102**: in print.
16. Pauling L, Wheland J. *J. Chem, Phys.* 1933; **1**: 606–617.
17. Kistiakowsky GB, Ruhoff JR, Smith HA, Vaughan WE. *J. Am. Chem. Soc.* 1936; **58**: 146–153.
18. (a) Pauling L, Wheland J. *J. Chem. Phys*. 1933; **1**: 362–374; (b) Wheland GW. *Resonance in Organic Chemistry.* Wiley: New York, 1955.
19. Hess BA, Schaad LJ. *J. Am. Chem. Soc.* 1971; **93**: 2413–2416.
20. (a) Häfelinger G. *Tetrahedron Lett.* 1971; 541–544; (b) Häfelinger G. *Tetrahedron* 1971; **27**: 4609–4636.
21. Schaad LJ, Hess BA Jr. *Chem. Rev.* 2001; **101**: 1465–1476.
22. Chung ALH, Dewar MJS. *J. Chem. Phys.* 1965; **42**: 756–766.
23. (a) Dewar MJS, deLlano C. *J. Am. Chem. Soc.* 1969; **91**: 789–795; (b) Dewar MJS, Gleicher GJ. *J. Am. Chem. Soc.* 1965; **87**: 685–692.
24. Hehre WJ, Ditchfield R, Radom L, Pople JA. *J. Am. Chem. Soc.* 1970; **92**: 4796–4801.
25. Hehre WJ, McIver RT, Pople JA, Schleyer PvR. *J. Am. Chem. Soc.* 1974; **96**: 7162.
26. Hess BA, Schaad LJ. *J. Am. Chem. Soc.* 1983; **103**: 7500.
27. Schleyer PvR, Jiao H. *Pure Appl. Chem.* 1996; **68**: 209–218.
28. Krygowski TM, Cyrański MK. *Chem. Rev.* 2001; **101**: 1385–1419.
29. (a) Kruzewski J, Krygowski TM. *Tetrahedron Lett.* 1972; 3839–3842; (b) Cyrañski MK, Krygowski TM. *Tetrahedron* 1996; **52**: 1713–1722; (c) Krygowski TM. *J. Chem. Inf. Comput. Sci.* 1993; **33**: 70–78; (d) Cyrański MK, Krygowski TM. *Tetrahedron* 1999; **55**: 6205–6210.
30. (a) Kruszewski J, Krygowski TM. *Tetrahedron Lett.* 1970; 319–324; (b) Kruszewski J, Krygowski TM. *Tetrahedron Lett.* 1972; 3839.
31. Julg A, Francois P. *Theor. Chim. Acta* 1967; **8**: 249–259.
32. Bird CW. *Tetrahedron* 1985; **41**: 1409–1414.
33. (a) Lazzeretti P. *Prog. Nucl. Magn. Reson. Spectrosc*. 2000; **36**: 1–88; (b) Pauling L. *J. Phys. Chem.* 1961; **4**: 673–674.
34. Flygare WH. *Chem. Rev.* 1974; **74**: 653–688.
35. Dauben HJ, Wilson JD, Laity JL. In *Non-Benzenoid Aromatics*, vol. 16-II, Snyder JP (ed). Academic Press: New York, 1971; 167–206.
36. (a) Seelwood PW. *Magnetochemistry* (2nd edn). Interscience: New York, 1956; (b) Pascal P. *Ann. Chim. Phys*. 1910; **19**: 5–70.
37. Bernstein HJ, Schneider WG. *Proc. Roy. Soc. London Ser. A* 1956; **236**: 515–528.
38. Haddon RC, Haddon VR, Jackman LM. *Topics Curr. Chem.* 1971; **16**: 103–220.
39. Elvidge JA, Jackman LM. *J. Chem. Soc.* 1961; 327–359.
40. Schleyer PvR, Maerker C, Dransfeld A, Jiao H, van Eikema Hommes NJR. *J. Am. Chem. Soc.* 1996; **118**: 6317–6318.
41. (a) Ditchfield R. *Chem. Phys. Lett.* 1972; **15**: 203–296; (b) Ditchfield R. *Mol. Phys*. 1974; **27**: 789–807; (c) Wolinski K, Hinton JF, Pulay P. *J. Am. Chem. Soc.* 1990; **112**: 8251–8260.
42. Gomes JANF, Mallion RB. *Chem. Rev.* 2001; **101**: 1349–1383.
43. Pople JA. *J. Chem. Phys.* 1956; **24**: 1111.
44. McConnell HM. *J. Chem. Phys.* 1957; **27**: 226–229.
45. Waugh JS, Fessenden RW. *J. Am. Chem. Soc.* 1957; **79**: 846–849; 1958; **80**: 6697.
46. Johnson CE, Bovey FA. *J. Chem. Phys.* 1958; **29**: 1012–1014.
47. Bovey FA. *Nuclear Magnetic Resonance Spectroscopy*. Academic Press: New York, 1969; 264–274.
48. London F. *J. Phys. Radium* 1937; **8**: 397–409.
49. McWeeny R. *Mol. Phys.* 1958; **1**: 311.
50. Haigh CW, Mallion RB. *Org. Magn. Reson.* 1972; **4**: 203–228.
51. (a) Häfelinger G. *Tetrahedron Lett.* 1979; 2011–2014; (b) Westermayer M, Häfelinger G, Regelmann C. *Tetrahedron* 1984; **40**: 1845–1854.
52. Barfield M, Grant DM, Ikenberry D. *J. Am. Chem. Soc.* 1975; **97**: 6956–6961.
53. (a) Blustin PH. *Mol. Phys.* 1978; **36**: 1441–1448; (b) Blustin PH. *Chem. Phys. Lett.* 1979; **64**: 507–510; (c) Blustin PH. *Mol. Phys.* 1980; **39**: 565–586.
54. (a) Hall GG, Hardisson A. *Proc. R. Soc. London Ser. A* 1962; **268**: 328–338; (b) Hall GG, Hardisson A, Jackman LM. *Tetrahedron, Suppl. 2* 1963; **19**: 101–109.
55. Roberts HGFf. *Theor. Chim. Acta* 1969; **15**: 63–72.
56. Long ER, Memory JD. *J. Chem. Phys.* 1974; **61**: 3865–3866.
57. Vogler H. *J. Am. Chem. Soc.* 1978; **100**: 7464–7471.
58. Zuschneid T, Fischer H, Handel T, Albert K, Häfelinger G. *Z. Naturforsch., Teil B* 2004; **59**: 1153–1176.
59. Günther H. *NMR-Spektroskopie* (2nd edn). Thieme: Stuttgart, 1983.
60. (a) Vogel E. *Hückel-Aromaten*. Rheinisch-Westfälische Akademie der Wissenschaften, Vortrag No. 228, Westdeutscher Verlag Opladen 1973; 1–40; (b) Vogel E. In *Current Trends in Organic Synthesis*, Nozaki H (ed). Pergamon Press: Oxford, 1983; 379–400.
61. (a) Mori N, Takemura T. *J. Chem. Soc., Perkin Trans. 2* 1973; 1259–1262; (b) Agarwal A, Barnes JL, Fletcher JL, McGlinchey, Sayer BG. *Can. J. Chem.* 1977; **55**: 2575–2581.
62. (a) Kuhr M, Musso H. *Angew. Chem. Int. Ed. Engl.* 1969; **8**: 147–148; (b) Kuhr M, Musso H. *Angew. Chem. Int. Ed. Engl.* 1971; **10**: 225–235; (c) Bock B, Kuhr M, Musso H. *Chem. Ber.* 1976; **109**: 1184–1194; (d) Brill G, Musso H. *Liebigs Ann. Chem.* 1979; 803–810; (e) Brotzeller U, Nyitrai J, Musso H. *Chem. Ber.* 1980; **113**: 3610–3620; (f) Eberhardt U, Deppisch B, Musso H. *Chem. Ber.* 1983; **116**: 119–135.
63. (a) Häfelinger G, Weissenhorn RG, Hack F, Westermayer G. *Angew. Chem. Int. Ed. Engl.* 1972; **11**: 725–726; (b) Häfelinger G, Hack F, Westermayer G. *Chem. Ber.* 1976; **109**: 833–847; (c) Häfelinger G, Hack F, Westermayer G. *Chem. Ber.* 1978; **111**: 1323–1329; (d) Esswein HD, Häfelinger G. *Z. Naturforsch., Teil B* 1978; **33**: 1026–1032; (e) Häfelinger G, Beyer M. *Chem. Ber.* 1981; **114**: 109–117; (f) Häfelinger G, Beyer M, Burry P, Eberle B, Ritter G, Westermayer G, Westermayer M. *Chem. Ber.* 1984; **117**: 895–903; (g) Häfelinger G, Ott G. *Liebigs Ann. Chem.* 1984; 1605–1615.
64. Zeitz K, Oberhammer H, Häfelinger G. *Z. Naturforsch., Teil B* 1977; **32**: 420–425.
65. Frisch MJ, Trucks GW, Schlegel HB, Scuseria GE, Robb MA, Cheeseman JR, Montgomery JA Jr, Vreven T, Kudin KN, Burant JC, Millam JM, Iyengar SS, Tomasi J, Barone V, Mennucci B, Cossi M, Scalmani G, Rega N, Petersson GA, Nakatsuji H, Hada M, Ehara M, Toyota K, Fukuda R, Hasegawa J, Ishida M, Nakajima T, Honda Y, Kitao O, Nakai H, Klene M, Li X, Knox JE, Hratchian HP, Cross JB, Adamo C, Jaramillo J, Gomperts R, Stratmann RE, Yazyev O, Austin AJ, Cammi R, Pomelli C, Ochterski JW, Ayala PY, Morokuma K, Voth GA, Salvador P, Dannenberg JJ, Zakrzewski VG, Dapprich S, Daniels AD, Strain MC, Farkas O, Malick DK, Rabuck AD, Raghavachari K, Foresman JB, Ortiz JV, Cui Q, Baboul AG, Clifford S, Cioslowski J, Stefanov BB, Liu G, Liashenko A, Piskorz P, Komaromi I, Martin RL, Fox DJ, Keith T, Al-Laham MA, Peng CY, Nanayakkara A, Challacombe M, Gill PMW, Johnson B, Chen W, Wong MW, Gonzalez C, Pople JA. *Gaussian 03, Revision C.02*. Gaussian: Wallingford, CT, 2004.
66. Roothaan CCJ. *Rev. Mod. Phys.* 1951; **23**: 69–89.
67. Hariharan PC, Pople JA. *Theor. Chim. Acta*, 1973; **28**: 213–222.
68. Dunning TH. *J. Chem. Phys.* 1989; **90**: 1007–1023.
69. Koch W, Holthausen MC. *A Chemist's Guide to Density Functional Theory.* Wiley-VCH: Weinheim, 1999.
70. (a) Becke AD. *J. Chem. Phys.* 1993; **98**: 5648–5652; (b) Stevens PJ, Devlin JF, Chabalowski CF, Frisch MJ. *J. Phys. Chem.* 1994; **98**: 11623–11627.
71. Møller C, Plesset MS. *Phys. Rev.* 1934; **46**: 618–622.

72. Knapp W. Thesis, University of Tübingen, 1987.
73. Church DF, Gleicher GJ. *J. Org. Chem.* 1976; **41**: 2327–2331.
74. Tsuzuki S, Tanabe K, Ozawa E. *J. Phys. Chem.* 1990; **94**: 6175–6179.
75. Schaefer T, Penner GH. *Chem. Phys. Lett.* 1985; **114**: 526–528.
76. Carreira LA, Towns TG, *J. Chem. Phys.* 1975; **63**: 5283–5286.
77. Caminati W, Vogelsanger B, Bauder A. *J. Mol. Spectrosc.* 1988; **128**: 384–398.
78. Bock CW, Trachtman M, George P, *Chem. Phys.* 1985; **93**: 431–443.
79. Pretsch E, Clerc T, Seibl J, Simon W. *Tabellen zur Strukturaufklärung Organischer Verbindungen mit Spektroskopischen Methoden*. Springer: Berlin, 1981.
80. (a) Musher JI. *J. Chem. Phys.* 1965; **43**: 4081–4083; (b) Musher JI. *Adv. Magn. Reson.* 1966; **2**: 177; (c) Musher JI. *J. Chem. Phys.* 1967; **46**: 1219–1221.
81. (a) Gaidis JM, West R. *J. Chem. Phys.* 1967; **46**: 1218–1219; (b) Gomes JANF. *Mol. Phys.* 1980; **40**: 765–769.
82. Agarwal A, Barnes JA, Fletcher JL, McGlinchey MJ, Sayer BG. *Can. J. Chem.* 1977; **55**: 2575–2581.
83. Lazzeretti P, Malagoli M, Zanasi R. *J. Mol. Struct. (Theochem)* 1991; **234**: 127–145.
84. Wannere CS, Schleyer PvR. *Org. Lett.* 2003; **5**: 605–608.
85. Viglione RG, Zanasi R, Lazzeretti P. *Org. Lett.* 2004; **6**: 2265–2267.